Rocky exoplanet characterization and atmospheres

L. Kaltenegger[1,2], Y. Miguel[1] and S. Rugheimer[2]

[1]*MPIA, Koenigstuhl 17, 69117 Heidelberg, Germany*
e-mail: kaltenegger@mpia.de
[2]*CfA, 60 Garden street, Cambridge 02138 MA, USA*

Abstract: A decade of exoplanet search has led to surprising discoveries, from giant planets close to their star, to planets orbiting two stars, all the way to the first extremely hot, rocky worlds with potentially permanent lava on their surfaces due to the star's proximity. Observation techniques have reached the sensitivity to explore the chemical composition of the atmospheres as well as physical structure of some detected gas planets and detect planets of less than 10 Earth masses (M_{Earth}), the so-called super-Earths, among them some that may potentially be habitable. Three confirmed non-transiting planets, and several transiting Kepler planetary candidates, orbit in the habitable zone (HZ) of their host star. The detection and characterization of rocky and potentially Earth-like planets is approaching rapidly with future ground and space missions that can explore the planetary environments by analysing their atmosphere remotely. This paper discusses how to characterize a rocky exoplanet remotely.

Introduction

The current status of exoplanet characterization shows a surprisingly diverse set of giant planets. For a subset of these, some properties have been measured or inferred using radial velocity (RV), micro-lensing, transits and astrometry. These observations have yielded measurements of planetary mass, orbital elements and the planetary radius and during the last few years, physical and chemical characteristics of the upper atmosphere of some of the transiting planets. Specifically, observations of transits, combined with RV information, have provided estimates of the mass, radius and density of a subset of these planets, ranging from giant planets to rocky planets such as Corot 7b (Léger *et al.* 2009) and Kepler 10b (Batalha *et al.* 2011). Due to a detection bias for both transiting and the RV method, most detected planets orbit extremely close to their host star and therefore receive high amounts of stellar irradiation and have subsequent high surface temperature. The first directly imaged exoplanet candidates around young stars show the improvement in direct detection techniques that are designed to resolve the planet and collect its photons. This can currently be achieved for widely separated young objects and has already detected exoplanets candidates (see e.g. Kalas *et al.* 2008; Marois *et al.* 2008; Lagrange *et al.* 2009).

Recent investigations of high precision RV data samples have shown that between 20 and 50% of all sample stars exhibit RV variations indicating the presence of super-Earths or ice giants (Howard *et al.* 2011). Among the hundreds of confirmed planets, already a few close by, low mass RV planets such as Gl 581 d (Udry *et al.* 2007), with minimum masses below 10 Earth masses, MEarth, orbit in the habitable zone (HZ) of their parent star. These close by planets provide excellent targets for future atmospheric exploration. Several Kepler transit planetary candidates from the February 2011 data release (Borucki *et al.* 2011) that are consistent with rocky models, orbit their host stars also in the HZ, providing first statistics of the number of planets and Earth-like planets (eta_{Earth}) (see e.g. Traub 2011) and a more complete sample is expected in the second Kepler data release in 2012.

The discovery of transiting planets with masses below 10 M_{Earth} and radii consistent with rocky planetary models, answered the important question if planets more massive than Earth could potentially be rocky. Ten M_{Earth} are used from formation theories as the upper limit for rocky planet formation, for comparison, Uranus has about 15 M_{Earth}. Above that mass the planet is thought to accumulate a substantial amount of gas that makes it akin to a gas giant, not a rocky planet with an outgassed atmosphere, what we use as the definition of Super-Earth here. Where exactly such a cut-off mass is – if it exists at all – an open question.

Recent discoveries by ground based, as well as the Corot and Kepler space-mission, found planets with radii below 2 Earth radii and masses below 10 M_{Earth} and densities akin to Neptune as well as Earth, suggesting that there is not one cut-off mass above which a planet is like Neptune and below which it is rocky like Earth or Venus. The first planets below 10 M_{Earth}, with both mass estimates and radius measurements, have provided a wide range of observed radii and densities (e.g., Seager *et al.* 2007; Sotin *et al.* 2007; Valencia *et al.* 2007; Grasset *et al.* 2009).
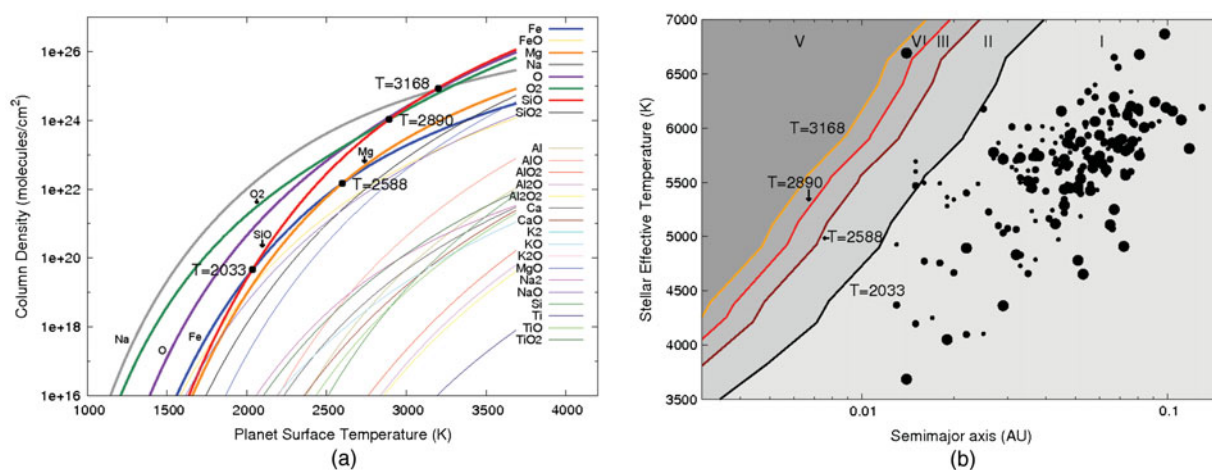
Fig. 1. Column densities of atmospheric gases as a function of the planet surface temperature (left panel). Temperatures where the most abundant gases change are indicated. Stellar effective temperature versus semi-major axis (right panel) (adapted from Miguel *et al.* 2011).

Especially in the mass range below $5M_{Earth}$, two planets in the multiple planet system, Kepler 11b and Kepler 11f (Lissauer *et al.* 2011), with 4.3 and 2.3 M_{Earth} have radii of 1.97 and 2.61 Earth radii and mean densities of 3.1 and 0.7 g/cm^3, respectively. These derived densities allow substantial envelopes of light gases for this mass range. Recent atmosphere observations for a 6.55 ± 0.98 Earth mass planet, GJ 1214 b (Charbonneau *et al.* 2009; Bean *et al.* 2011; Désert *et al.* 2011), with a mean density of 1.8 g/cm^3, indicates either hazes or high cloud cover in an expanded atmosphere (Miller-Ricci *et al.* 2012). For comparison Neptune has a mean density of 1.6 g/cm^3, Earth a mean density of 5.5 g/cm^3.

Observing mass and radius alone cannot break the degeneracy of a planet's nature due to the effect of an extended atmosphere that can block the stellar light and increase the observed planetary radius significantly. Even if a unique solution would exist, planets with similar density, such as Earth and Venus, present very different planetary environments in terms of habitable conditions. Therefore, the question refocuses on atmospheric features to characterize a planetary environment. Future space missions have the explicit purpose of detecting other Earth-like worlds, analysing their characteristics, determining the composition of their atmospheres, investigating their capability to sustain life as we know it and searching for signs of life. They also have the capacity to investigate the physical properties and composition of a broader diversity of planets, to understand the formation of planets and interpret potential biosignatures.

In this paper, we discuss how we can read a planet's spectral fingerprint and characterize if it is potentially habitable. In section 1, we discuss the hot, close in planetary sample, in section 2, the first steps to detect a habitable planet, set biomarker detection in context and focuses on low resolution biomarkers in the spectrum of an Earth-like planet are discussed. In section 3, we discuss spectral evolution of a habitable planet, abiotic sources of biomarkers and Earth's spectra around different host stars, and section 4 summarizes the article.

Hot rocky exoplanets

Exoplanet surveys have already discovered the first rocky, strongly irradiated exoplanets: Corot 7b (Léger *et al.* 2009) and Kepler 10b (Batalha *et al.* 2011). A whole population of hot planets with minimum masses below 10 Earth masses, consistent with rocky planet models (super-Earths) has already been detected. In the Kepler February 2011 data release (Borucki *et al.* 2011), the Kepler team presented 997 stars with a total of 1235 planetary candidates. Six hundred and fifteen of these objects have radii consistent with rocky planetary models (smaller than 2 Earth radii within measurement errors) and a subsample of 193 might have extremely high temperatures on their surfaces ($T_P > 1000$ K), due to stellar irradiation alone, assuming a rocky planet model with a Bond albedo of 0.01 (Miguel *et al.* 2011).

Such extreme conditions are not seen on any planet in our Solar System and therefore the potential atmospheric composition of these hot super-Earths remains largely unknown. For temperatures above 1000 K, the surface of a rocky planet would be covered with a magma ocean which will vapourize, forming an outgassed atmosphere. Schaefer & Fegley (2009) modelled this process for Corot 7b, showing a silicate atmosphere is possible for such hot objects. Miguel *et al.* (2011) developed a simple approach linking the observable data of a planet (radius, semi-major axis and stellar effective temperature) to the atmospheric composition for such hot planets. The results were applied to the hot, potentially rocky, planets in the Kepler sample computing the chemical equilibrium between the melt and vapour in a magma exposed at temperatures between 1000 and 3500 K using the MAGMA-code (Fegley & Cameron 1987; Schaefer & Fegley 2004).

The resulting column densities of the atmospheric gases outgassed for a planet of 10 Earth masses as a function of the surface temperature are shown in Fig. 1(a) with the most abundant gases being Fe, Mg, Na, O, O_2 and SiO. The abundance of each gas in the atmosphere depends on the surface temperature. The temperatures where the abundance of
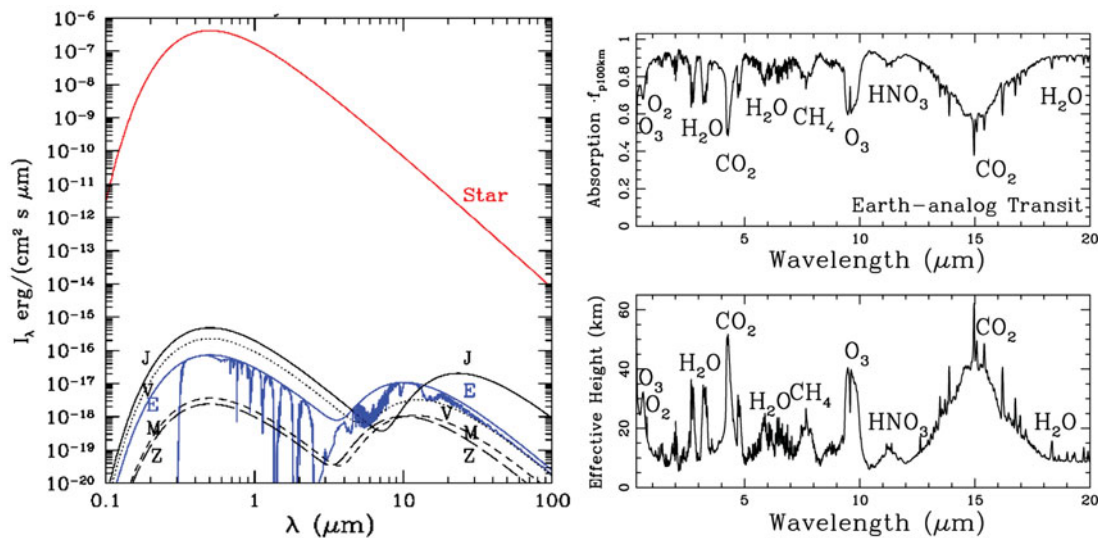
Fig. 2. Model of our Solar System (left) (assumed here to be Black Bodies with Earth spectrum shown). Synthetic transmission spectra (right) of the Earth from UV to IR shown. The intensity is given as a fraction of solar intensity as well as the relative height in the atmosphere. The atmospheric features are indicated (Kaltenegger *et al.* 2011).

the most important gases change significantly are indicated in the figures, and define different atmospheric types (Miguel *et al.* 2011). Fig. 1(b) shows the stellar effective temperature versus the planet's distance to its star. Kepler planetary candidates with $T_p > 1000$ K are also shown in different point sizes according to their radius: 2–2.5 Earth radii (large points), 1.5–2 Earth radii (medium points) and candidates with $R_p < 1.5$ Earth radii (small points). According to these results, there are five types of initial atmospheres for hot rocky planets (for details, see Miguel *et al.* 2011).

Characterize a habitable planet (learning from Earth)

In the next few years, ground- and space-based missions will give us statistics on the number, size, period and orbital distance of planets, extending to terrestrial planets on the lower mass range end as a first step, while future space missions are designed to characterize their atmospheres. A temperate planet is a very faint, small object close to a very bright and large object, its parent star. For directly imaging planets, in the visible part of the spectrum we observe the starlight, reflected off the planet, in the IR we detect the planets own emitted flux. The Earth–Sun intensity ratio is about 10^{-7} in the thermal infrared (IR) (~ 10 μm) and about 10^{-10} in the visible (~ 0.5 μm) (see Fig. 2). Nevertheless, the contrast ratio of hot extrasolar Giant planets (EGP) to their parent stars as well as the contrast ratio of a planet to a smaller parent star is much more favourable, making Earth-like planets around small stars very interesting targets.

Low mass Main Sequence M dwarfs are the most abundant stars in the galaxy, representing about 75% of the total stellar population. Many planets including potentially rocky planets within the HZ, such as Gl581d (see e.g. Kaltenegger *et al.* 2011; von Paris *et al.* 2010; Wordsworth *et al.* 2011), are thus likely to

be found in the near future. These will provide excellent targets (see e.g. Scalo *et al.* 2007) that can be probed for atmospheric components, especially for hot planets with extended atmospheres.

Different strategies exist to characterize a planet's atmosphere: direct detection resolves the planet and star individually, and transmission as well as secondary eclipse measurements subtract the stellar light from a combined star–planet detection. Future telescopes will allow for direct detection in close orbits for close by stars.

A spectral fingerprint of an Earth-like atmosphere

The atmosphere of a planet contains the detectable information to explore the planetary environment remotely. On Earth some atmospheric species exhibiting noticeable spectral features in the planet's spectrum result directly or indirectly from biological activity: the main ones are O_2, O_3, CH_4 and N_2O (see Fig. 2). Figure 2 shows the detectable features in the planet's reflection, emission and transmission spectrum using the Earth itself as a proxy for observations and model fits to data of spectra of the Earth (Kaltenegger *et al.* 2007; Kaltenegger & Traub 2009). CO_2 and H_2O are in addition important as greenhouse gases in a planet's atmosphere and potential sources for high O_2 concentration from photosynthesis. Sagan *et al.* (1993) analysed a spectrum of the Earth taken by the Galileo probe, searching for signatures of life and concluded that the large amount of O_2 and the simultaneous presence of CH_4 traces are strongly suggestive of biology for a planet around a Sun-like star.

Figure 3 shows observations and model fits to spectra of the Earth in three wavelength ranges (Kaltenegger *et al.* 2007). The data shown in Fig. 3 (left) are the visible Earthshine spectrum (Woolf *et al.* 2002), (centre) the near-IR (NIR) Earthshine spectrum (Turnbull *et al.* 2006) and (right) the thermal IR spectrum of Earth as measured by a spectrometer en route to
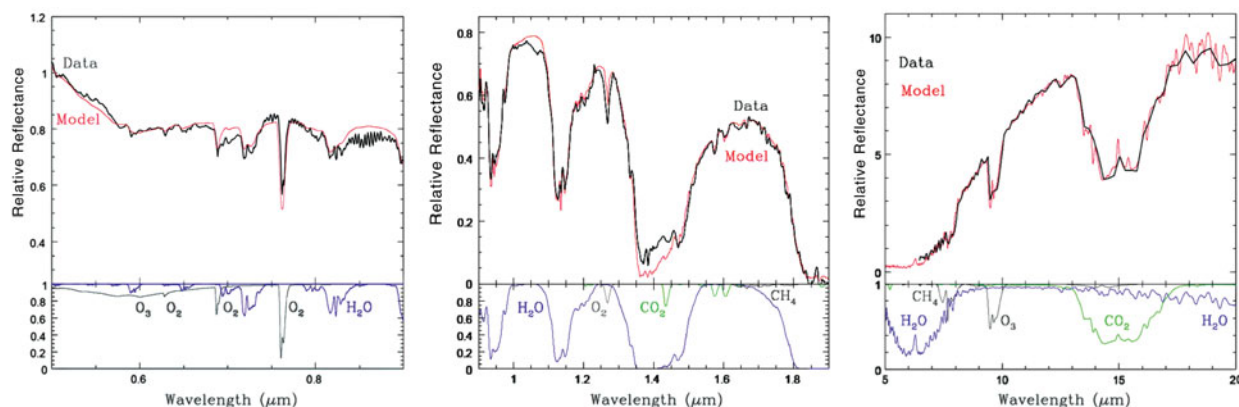
Fig. 3. Observed reflectivity spectrum in the visible (Woolf *et al.* 2002) (top), NIR (Turnbull *et al.* 2006) (middle) and emission spectrum in the IR (Christensen & Pearl 1997) (bottom panel) of the integrated Earth, as determined from Earthshine and space, respectively. The data are shown in black and the SAO model in red. The reflectivity scale is arbitrary (Kaltenegger *et al.* 2007).

Mars (Christensen & Pearl 1997). The data are shown in black and the SAO model in red. In each case, the constituent gas spectra in a clear atmosphere are shown in the bottom panel, for reference.

Our search for signs of life in exoplanets is based on the assumption that extraterrestrial life shares fundamental characteristics with life on Earth, in that it requires liquid water as a solvent and has a carbon-based chemistry (see e.g. Brack 1993; DesMarais *et al.* 2002). Life based on a different chemistry is not considered here because these life forms would produce signatures in their atmosphere that are so far unknown. Therefore, we assume extraterrestrial life is similar to life on Earth in its use of the same input and output gases, and that it exists out of thermodynamic equilibrium (Lovelock 1975).

The viewing geometry results in different flux contribution of the overall detected signal from the bright and dark side, for the reflected light, the terminator region for transmitted light and the planet's hot and cold regions for the emitted flux. Biosignatures are used here to mean detectable species, or set of species, whose presence at significant abundance strongly suggests a biological origin (e.g. couple $CH_4 + O_2$, or $CH_4 + O_3$). It is their quantities and detection along with other atmospheric species, in a certain context (for instance the properties of the star and the planet) that points toward a biological origin. O_2, O_3 with a reducing gas such as CH_4 are good biosignatures that can be detected by a low-resolution (resolution < 80) spectrograph.

Visible and NIR as well as IR spectral regions contain the signature of atmospheric gases that can be observed with low resolution and can indicate habitable conditions and, possibly, the presence of a biosphere: CO_2, H_2O, O_3, CH_4 and N_2O in the thermal IR, and H_2O, O_3, O_2, CH_4 and CO_2 in the visible to NIR (see e.g. DesMarais *et al.* 2002; Meadows & Seager 2010; Kaltenegger *et al.* 2011, and references therein for detailed reviews). The presence or absence of these spectral features (detected collectively) will indicate similarities or differences with the atmospheres of terrestrial planets, and its astrobiological potential. Note that the presence of biogenic

gases such as $O_2/O_3 + CH_4$ may imply the presence of an active biosphere, but their absence does not imply the absence of life. Life existed on Earth before the interplay between oxygenic photosynthesis and carbon cycling produced an oxygen-rich atmosphere (see section 4).

Characterizing planetary environment

It is relatively straightforward to remotely ascertain Earth is a habitable planet, replete with oceans, a greenhouse atmosphere, global geochemical cycles, and life if one has data with arbitrarily high signal-to-noise and spatial and spectral resolution. The interpretation of observations of other planets with limited signal-to-noise ratio and spectral resolution as well as absolutely no spatial resolution, as envisioned for the first generation instruments, will be far more challenging and implies that we need to gather information on the planet environment to understand what we will see. After detection, we will focus on the main properties of the planetary system, its orbital elements as well as the presence of an atmosphere using the light curve of the planet (Selsis *et al.* 2003; Gaidos & Williams 2004; Moskovitz *et al.* 2009; Wordsworth *et al.* 2011) or/and a crude estimate of the planetary nature using very low-resolution information (three or four channels) (see e.g. Traub *et al.* 2003).

Knowing the temperature and planetary radius is crucial for the general understanding of the physical and chemical processes occurring on the planet (tectonics and hydrogen loss to space). Presently, radius measurements can only be performed when the planet transits in front of its parent star, by an accurate photometric technique. If the secondary eclipse of the transiting planet can be observed (when the planet passes behind the star) or the planet can be imaged, then the thermal emission of the planet can be measured, allowing the retrieval of mean brightness temperature T_b, and the radius from the IR flux. One can also calculate the stellar energy of the star F_{star} that is received at the measured orbital distance. The surface temperature of the planet at this distance depends on its albedo and on the greenhouse warming by atmospheric compounds. However, with a low-resolution spectrum of the
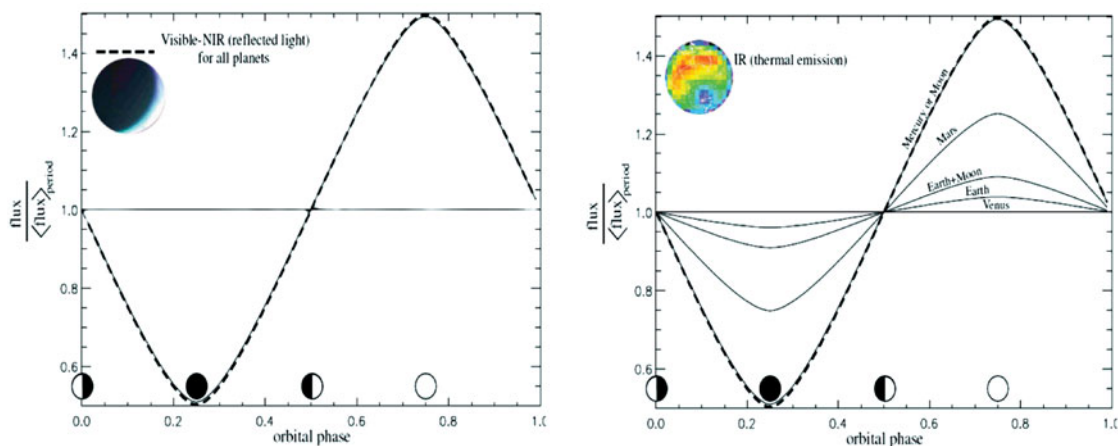
Fig. 4. Orbital light curve for black body planets in a circular orbit with null obliquities, with and without an atmosphere in the visible (top) and thermal IR (bottom) (after Selsis *et al.* 2003).

thermal emission, the mean effective temperature and the radius of the planet can be obtained.

The accuracy of the radius and temperature determination will depend on the quality of the fit (and thus on the sensitivity and resolution of the spectrum), the precision of the Sun–star distance, the cloud coverage and also the distribution of brightness temperatures over the planetary surface. Assuming the effective temperature of our planet was radiated from the uppermost cloud deck at about 12 km would introduce about 2% error on the derived Earth radius. For transiting planets, for which the radius is known, within a certain measurement error, the measured IR flux can directly be converted into a brightness temperature that will provide information on the temperature of the atmospheric layers responsible for the emission.

If only the mass of non-transiting planets can be measured (by RV and/or astrometric observations), a first estimate of the radius can be made by assuming a bulk composition of the planet which can then be used to convert IR fluxes into temperatures. The ability to associate a surface temperature with the spectrum relies on the existence and identification of spectral windows probing the surface or the same atmospheric levels. Such identification is not trivial. For an Earth-like planet there are some atmospheric windows that can be used in most of the cases, especially between 8 and 11 μm as seen in Fig. 2. This window would, however, become opaque at high H_2O partial pressure (e.g. the inner part of the HZ where a lot of water is vapourized) and at high CO_2 pressure (e.g. a very young Earth or the outer part of the HZ).

The orbital flux variation in the IR can distinguish planets with and without an atmosphere in the detection phase (see also Selsis *et al.* 2003; Gaidos & Williams 2004). Strong variation of the thermal flux with phase reveals a strong difference in temperature between the day and night hemisphere of the planet, and is a consequence of the absence of a dense atmosphere. In such a case, estimating the radius from the thermal emission is made difficult because most of the flux received comes from the small and hot substellar area. The ability to retrieve the radius would depend on the assumptions

that can be made about the orbit geometry and the rotation rate of the planet. In most cases, degenerate solutions will exist. When the mean brightness temperature, T_b, is stable along the orbit, the estimated radius is more reliable. The radius can be measured at different points of the orbit and thus for different values of T_b, which should allow an estimate of the error.

The mean value of T_b estimated over an orbit can be used to estimate the Bond albedo of the planet, its reflectivity, through the balance between the incoming stellar radiation and the outgoing IR emission. In the visible ranges, the reflected flux allows us to measure the product of Bond Alebdo times planetary area (a small but reflecting planet appears as bright as a big but dark planet).

The thermal light curve (i.e. the integrated IR emission measured at different position on the orbit) exhibits smaller variations due to the phase (whether the observer sees mainly the day side or the night side) and to the season on a planet with an atmosphere than the corresponding visible lightcurve variations. Therefore, planets with dense atmospheres can be distinguished from airless or Mars-like planets by the amplitude of the observed variations of T_b (see Fig. 4).

As a second step a higher resolution spectrum will be used for interesting planetary targets to identify the compounds of the planetary atmosphere, constrain the temperature and radius of the observed exoplanet. In that context, we can test if we have an abiotic explanation of all compounds seen in the atmosphere of such a planet. If we do not, we can begin to consider the exciting biotic hypothesis.

The HZ

Different aspects of what determines the boundaries of the HZ have been discussed broadly in the literature. Habitability and the HZ are functions of the stellar flux at the planet's location as well as the planet's atmospheric composition. The latter determines the albedo and the greenhouse effect in the atmosphere. The inner and outer boundaries of the HZ differ for clear and cloudy conditions because the overall planetary albedo A, is a function of the chemical composition of the clear atmosphere as well as the fraction of clouds, $A = A_{clear} + A_{cloud}$.

The main differences among studies of the HZ are the imposed chemical composition and cloud fraction of the planet's atmosphere. Examples of atmospheres with different chemical compositions include the original $CO_2/H_2O/N_2$ model with a water reservoir (e.g. Earth's), or model atmospheres with high H_2/He concentrations (Pierrehumbert & Gaidos 2011) or limited water supply (Abe *et al.* 2011). Two concepts are commonly used throughout the literature for cloud-free (see Kasting *et al.* 1993) and cloudy atmospheres (Selsis *et al.* 2007). According to this model, the HZ is an annulus around a star where a rocky planet with a $CO_2/H_2O/N_2$ atmosphere and sufficiently large water content (such as in Earth) can host liquid water permanently on a solid surface. This definition of the HZ assumes that the planet is rocky, water is present, the main atmospheric composition is $CO_2/H_2O/N_2$, and the abundance of H_2O and CO_2 in the atmosphere is regulated by a geophysical cycle similar to that of Earth, resulting in an H_2O- and CO_2-dominated atmosphere on the inner and the outer edges of the HZ, respectively. Between those limits on a geological active planet, climate stability is provided by a feedback mechanism in which atmospheric CO_2 concentration varies inversely with planetary surface temperature. In this definition, the locations of the two edges of the HZ are determined based on the equilibrium temperature of the planet (see e.g. Kasting *et al.* 1993; Selsis *et al.* 2003; Kaltenegger & Sasselov 2011).

As shown by Selsis *et al.* (2003) and from the cases studied in Kasting *et al.* (1993), for a star with luminosity L and an effective temperature T_{Star} between 3700 and 7200 K, the inner and outer boundaries of the HZ (l_{in}, l_{out}) can be obtained from

$$l_x(T_{Star}, L_{Star}) = (l_{xSum} - a_x T_S - b_x T_S^2)\left(\frac{L_{Star}}{L_{Sum}}\right)^{1/2}. \quad (1)$$

In this equation, l_x (l_{in} and l_{out}) is in AU, $a_{in} = 2.7619 \times 10^{-5}$, $b_{in} = 3.8095 \times 10^{-9}$, $a_{out} = 1.3786 \times 10^{-4}$, $b_{out} = 1.4286 \times 10^{-9}$ and T_S (K) $= T_{Star}$(K) $- 5700$. As indicated by eq. (1), the extrapolated boundaries of the HZ are functions of the input parameter l_{x-Sun}, the inner and outer limits of the Sun's HZ. As mentioned earlier, these limits are model dependent and different for different values of cloud fraction and atmosphere composition. In this study, we consider the values of l_{in-Sun} and $l_{out-Sun}$ corresponding to the following scenarios.

For the inner boundary of the Sun's HZ (Fig. 1), we consider the water-loss limit ($T_{surf} = 373$ K) of the HZ of our Solar System for 0 and 50% cloud fraction (Kasting *et al.* 1993; Selsis *et al.* 2003). In this scenario, the value of l_{in-Sun} is equal to 0.95 and 0.76 AU for 0 and 50% cloud fractions (f), respectively. The outer boundary denotes the distance from the star where the maximum greenhouse effect fails to keep CO_2 from condensing permanently, leading to runaway glaciation. For the outer boundary of the Sun's HZ, we consider the theoretical values of $l_{out-Sun} = 1.67$ and 1.95 AU corresponding to a cloud-free and 50% cloud-fraction CO_2 atmosphere. We choose those model values because they correspond to the empirical limits based on the initial Solar flux received
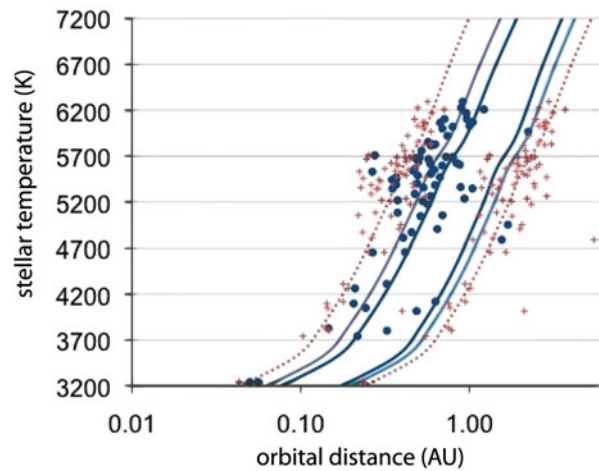

Fig. 5. Extent of the HZ for water loss limit for 0 and 50% cloud coverage (inner limits) and 100% cloud coverage (outer limit dashed line) and position of potentially habitable Kepler planetary candidates in the HZ, individual HZ limits are indicated with crosses (Kaltenegger & Sasselov 2011).

at the position of Venus and Mars with $l_{in-Sun} = 0.75$ AU and $l_{out-Sun} = 1.77$ AU, respectively (see Kasting *et al.* 1988, 1993 for details). Note that in the empirical Mars limit, the value of the outer boundary of the HZ is biased by Mars' small size, which did not allow this planet to maintain a dense greenhouse atmosphere. At the limits of the HZ, the Bond albedo of a habitable planet is fully determined by its atmospheric composition and depends on the spectral distribution of the stellar irradiation.

In this definition, the two edges of the HZ (see Fig. 5), depend on the Bond albedo of the planet A, the luminosity of the star L_{star}, the planet's semi-major axis D, as well as the eccentricity e, of the orbit, and in turn the average stellar irradiation at the planet's location. A more eccentric orbit increases the annually averaged irradiation proportional to $(1 - e^2)^{1/2}$ (Williams & Pollard 2002). However, the limits of the HZ are known qualitatively, more than quantitatively. This uncertainty is mainly due to the complex role of clouds and three-dimensional climatic effects not yet included in the modelling. Thus, planets slightly outside the computed HZ could still be habitable, while planets at habitable orbital distance may not be habitable because of their size or chemical composition. Subsurface life that could exist on planets with very different surface temperatures is not considered here, because of the lack of remotely detectable atmospheric to assert habitability.

Applying this definition to the Kepler February 2011 data release, assuming circular orbits and albedo corresponding to 50% cloud coverage (consistent with the empirical 'Venus'-limit of the HZ), leads to 27 Kepler planetary candidates in the HZ. Among those are three planetary candidates with radii smaller than two Earth radii (Kaltenegger & Sasselov 2011). The potentially rocky Kepler planet candidates in multiple systems are especially interesting objects because their mass could be determined using transit time variations to calculate a
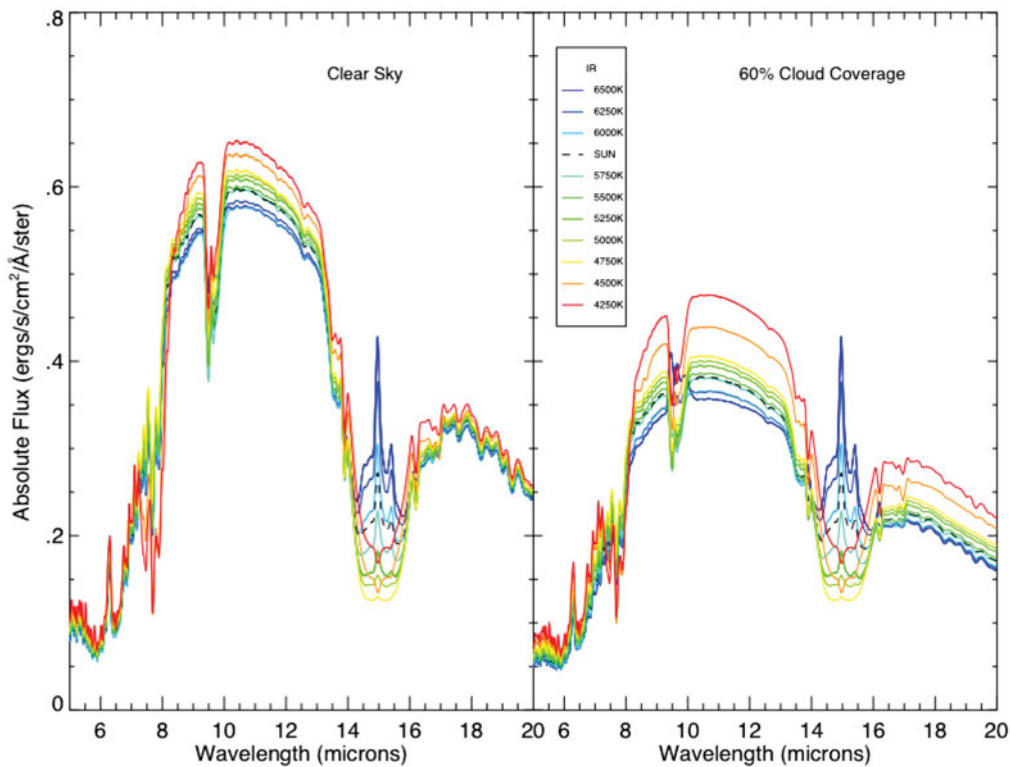
Fig. 6. Clear sky model (left) and 60% cloud coverage (right) of the IR spectral region at a resolution of 25 (corresponding to proposed resolution of future space missions) for an Earth-analogue planet around FGK stars (Rugheimer *et al.* submitted).

mean density and potentially confirm high density and rocky characteristics.

Due to the large mean distance to the Kepler stars and planets, the characterization of the planets atmospheres will not be in the near future, although it is an excellent mission to derive statistics. Small planets detected around stars close to the Sun will provide the planetary targets that can be followed up with the next generation of ground- and space-based telescopes.

Characterization of planetary spectra

Influence of host-stars

The range of characteristics of planets is likely to exceed our experience with the planets and satellites in our own Solar System by far. Models of planets more massive than our Earth – rocky super-Earths – need to consider the changing atmosphere structure, as well as the interior structure of the planet (see e.g. Seager *et al.* 2007; Sotin *et al.* 2007; Valencia *et al.* 2007; Grasset *et al.* 2009). Also, Earth-like planets orbiting stars of different spectral type might evolve differently. Modelling these influences will help to optimize the design of the proposed instruments to search for Earth-like planets.

Using a numerical code that simulates the photochemistry of a wide range of planetary atmospheres several groups (Selsis 2000; Segura *et al.* 2003, 2005; Grenfell *et al.* 2007; Pallé *et al.* 2009) have simulated the atmospheric composition of a replica of our planet orbiting different types of star: F-type star (more massive and hotter than the Sun) and a K-type star (smaller

and cooler than the Sun). The models assume similar background composition of the atmosphere as well as similar strength of biogenic sources.

For an Earth-analogue planet around a spectral grid of host stars ranging in $6250\,K < T_{eff} < 6500\,K$ at a resolution $\lambda/\Delta\lambda = 25$ Fig. 6 shows the IR emergent modelled spectrum for F, G and K stars (Rugheimer *et al.* submitted) for a clear sky emergent spectra as well as a 60% global cloud coverage analogous to Earth (40% 1 km cloud layer, 40% 6 km cloud layer and 20% 12 km cloud layer). The spectra are presented relative to the planet's surface temperature black body. Clouds have high reflection in the visible. In the IR, the temperature difference between the emitting/absorbing layer and the surface determines the strength of the spectral feature. Since on Earth clouds emit at temperatures generally colder than the surface, they can increase as well as reduce the depth of features in the IR as can be seen in the cases of CO_2 at 15 μm, O_3 at 9.6 μm and CH_4 feature at 7.7 μm.

A planet orbiting a K star has a thin O_3 layer, compared with Earth's one, but still exhibits a deep O_3 absorption: indeed, the low UV flux is absorbed at lower altitudes than on Earth which results in a less efficient warming (because of the higher heat capacity of the dense atmospheric layers). Therefore, the ozone layer is much colder than the surface and this temperature contrast produces a strong feature in the thermal emission. The process works the other way around in the case of an F-type host star. Here, the ozone layer is denser and warmer than the terrestrial one, exhibiting temperatures about as high as the surface temperature. Thus, the resulting low temperature
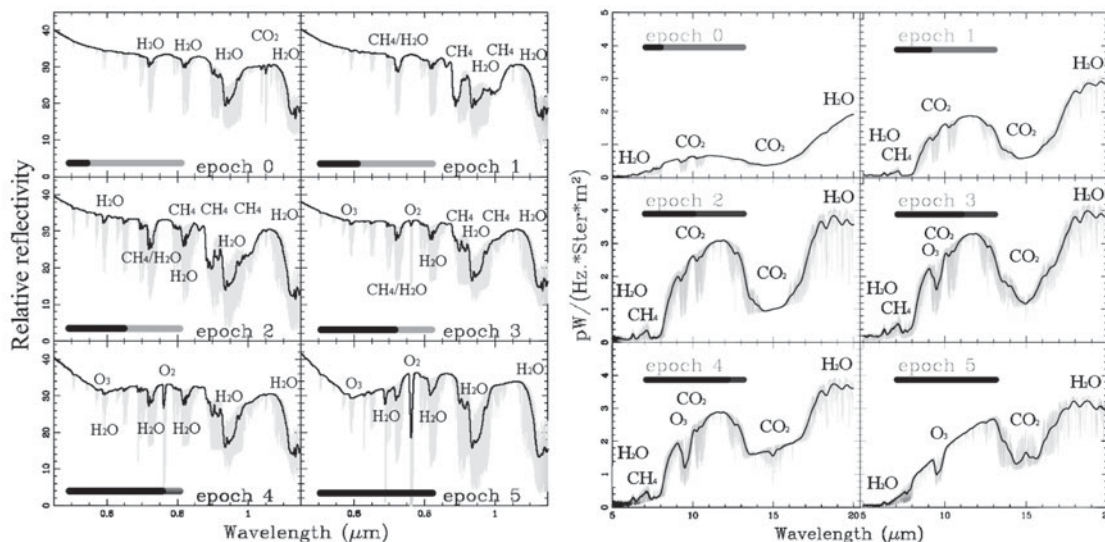
Fig. 7. The visible to NIR (top) and mid-IR (bottom) spectral features on an Earth-like planet change considerably over its evolution from a CO_2-rich (epoch 0) to a CO_2/CH_4-rich atmosphere (epoch 3) to a present-day atmosphere (epoch 5). The bold lines show spectral resolution of 80 and 25 comparable with the proposed visible TPF and Darwin/proposed future space missions (TPF-I) mission concept, respectively (Kaltenegger *et al.* 2007).

contrast produces only a weak and barely detectable feature in the IR spectrum. This comparison shows that planets orbiting G (solar) and K-type stars may be better candidates for the search for the O_3 signature than planets orbiting F-type stars (see Fig. 6). This result is promising since G- and K-type stars are much more numerous than F-type stars, the latter being rare and affected by a short lifetime (< 1 Gyr). Due to the hot stratosphere for all F-type stars ($T_{eff} > 6000$ K), the CO_2 absorption feature at 15 µm has a prominent central emission peak visible. The central peak can be thought of as an indirect feature indicating a temperature inversion in the atmosphere (see also Selsis 2000). The O_3 feature at 9.6 µm is increasingly difficult to resolve for hotter stellar types, despite increasing ozone abundance, due to the hotter stratosphere of the F-type stars (see also Selsis 2000). The CH_4 feature at 7.7 µm, while visible for F- and G-type stars, is more prominent in the late *K* dwarfs (4500 and 4250 K) than in hotter stars due to its higher abundance from a lower UV environment.

Evolution of biomarkers over geological times on Earth

One crucial factor in interpreting planetary spectra is the point in the evolution of the atmosphere when its biomarkers and its habitability become detectable. The spectrum of the Earth has not been static throughout the past 4.5 Ga. This is due to the variations in the molecular abundances, the temperature structure and the surface morphology over time. At about 2.3 Ga oxygen and ozone became abundant, affecting the atmospheric absorption component of the spectrum. At about 0.44 Ga, an extensive land plant cover followed, generating the red chlorophyll edge in the reflection spectrum. The composition of the surface (especially in the visible), the atmospheric composition and temperature–pressure profile can all have a significant influence on the detectability of a signal. Figure 7

shows theoretical visible and mid-IR spectra of the Earth at six epochs during its geological evolution (Kaltenegger *et al.* 2007). The epochs are chosen to represent major developmental stages of the Earth, and life on Earth. If an extrasolar planet is found with a corresponding spectrum, we can use the stages of evolution of our planet to characterizing it, in terms of habitability and the degree to which it shows signs of life. Furthermore, we can learn about the evolution of our own planet's atmosphere and possibly the emergence of life by observing exoplanets in different stages of their evolution. Earth's atmosphere has experienced dramatic evolution over 4.5 billion years, and other planets may exhibit similar or greater evolution, and at different rates. Figure 7 shows epochs that reflect significant changes in the chemical composition of Earth's atmosphere. The oxygen and ozone absorption features could have been used to indicate the presence of biological activity on Earth anytime during the past 50% of the age of the solar system. Different signatures in the atmosphere are clearly visible over Earth's evolution and observable with low resolution. The spectral resolution required for optimal detection of habitability and biosignatures has to be able to detect those features on our own planet for the dataset we have over its evolution.

Spectra of the Earth exploring temperature sensitivity (hot house and cold scenario) and different singled out stages of its evolution (e.g. Pavlov *et al.* 2000; Schindler & Kasting 2000; Traub & Jucks 2006) produce a variety of spectral fingerprints for our own planet. Strong volcanism (Kaltenegger *et al.* 2011), as well as other geochemical cycles could also be detected in a planet's spectrum (Domagal-Goldman *et al.* 2011; Kaltenegger & Sasselov 2011).

Those spectra will be used as part of a grid to characterize any exoplanets found and influences the design requirements for a spectrometer to detect habitable planets.

Surface and red-edge features

Although they efficiently absorb the visible light, photosynthetic plants have developed strong IR reflection (possibly as a defence against overheating and chlorophyll degradation) resulting in a steep change in reflectivity around 700 nm, called the red-edge. The primary molecules that absorb the energy and convert it to drive photosynthesis (H_2O and CO_2 into sugars and O_2) are chlorophyll A (0.450 μm) and B (0.680 μm). The exact wavelength and strength of the spectroscopic 'vegetation red-edge' (VRE) depends on the plant species and environment. On Earth around 440 million years ago (Schopf 1993; Pavlov *et al*. 2003), an extensive land plant cover developed, generating the red chlorophyll edge in the reflection spectrum between 700 and 750 nm. Averaged over a spatially unresolved hemisphere of Earth, the additional reflectivity of this spectral feature is typically a few percent (see also Arnold *et al*. 2002; Montanes-Rodriguez *et al*. 2005; Cowan *et al*. 2009). Several groups (Woolf *et al*. 2002; Turnbull *et al*. 2006; Montanes-Rodriguez *et al*. 2007) have measured the integrated Earth spectrum via the technique of Earthshine, using sunlight reflected from the non-illuminated, or 'dark', side of the moon. Earthshine measurements have shown that detection of Earth's VRE is feasible if the resolution is high and the cloud coverage is known, but is made difficult owing to its broad, essentially featureless spectrum and cloud coverage. Space-based EPOXI measurements have shown similar results (Cowan *et al*. 2009; Livengood *et al*. 2011).

Our knowledge of the reflectivity of different surface components on Earth – such as deserts, ocean and ice – helps in assigning the VRE of the Earthshine spectrum to terrestrial vegetation. Earth's hemispherical-integrated VRE signature is very weak, but planets with different rotation rates, obliquities, land–ocean fraction and continental arrangement may have lower cloud-cover and higher vegetated fraction (see e.g. Seager & Ford 2002). Knowing that other pigments exist on Earth and that some minerals can exhibit a similar spectral shape around 750 nm (Seager *et al*. 2005), the detection of the red-edge of the chlorophyll on exoplanets, despite its interest, will not be unambiguous.

Picking the most different reflecting surfaces (snow with a high albedo and sea with an extremely low albedo) shows the maximum effect surface coverage could have on the amount of light reflected from an exoplanet – assuming the whole planet surface is covered with that one material, the surface area is the same, and also artificially assuming similar cloud coverage and atmospheres for comparison. If similar photosynthesis would evolve on a planet around other stellar types, the possible different types of a vegetation spectral signature have been modelled (Kiang *et al*. 2007). Those signatures will be difficult to verify through remote observations as being of biological origin.

Clouds reduce the relative depths, full widths and equivalent widths of spectral features, weakening the spectral lines in the visible (Kaltenegger *et al*. 2007). In the thermal IR, clouds emit at temperatures that are generally colder than the surface and can both enhance or reduce the depth of the absorption features, while in the visible the clouds themselves have different spectrally dependent albedo that further influence the overall shape of the spectrum.

If one could record the planet's signal with a very high time resolution (a fraction of the rotation period of the planet) and SNR, one could determine the overall contribution of clouds to the signal (Pallé *et al*. 2008). During each of these individual measurements, one has to collect enough photons for a high individual SNR per measurement to be able to correlate the measurements to the surface features, what precludes this method for first-generation missions that will observe a minimum of several hours to achieve an SNR of 5–10. For Earth (Cowan *et al*. 2009; Pallé *et al*. 2008; Livengood *et al*. 2011) such high SNR measurements show a correlation to Earth's surface feature because the individual measurements are time resolved as well as have an individual high SNR, making it a very interesting concept for future generations of missions.

Summary

Spectroscopy of the atmosphere of extrasolar planets allows us to remotely explore a planets environment, to distinguish Mini-Neptunes from rocky Super-Earths, and to explore atmospheric compositions as well as search for indications for habitability. Any information we collect on habitability is only important in a context that allows us to interpret, what we find. To search for signs of life we need to understand how the observed atmosphere physically and chemically works. Knowledge of the temperature and planetary radius is crucial for the general understanding of the physical and chemical processes occurring on the planet. These parameters as well as an indication of habitability can be determined with low resolution spectroscopy and low photon flux, as assumed for first generation space missions. The combination of spectral information in the visible (starlight reflected of the planet) as well as in the mid-IR (planet's thermal emission) allows a confirmation of atmospheric species, a more detailed characterization of individual planets, but also to explore a wide domain of planet diversity. Being able to measure the outgoing shortwave and longwave radiation, as well as their variations along the orbit, and to determine the albedo and identify greenhouse gases would, in combination, allow us to explore the climate system at work on other worlds. Ultimately future missions will allow us probe planets similar to our own for habitable conditions.

Acknowledgements

References

Abe, Y., Abe-Ouchi, A., Sleep, N.H. & Zahnle, K.J. (2011). Habitable zone limits for dry planets. *Astrobiology* **11**(5), 443–460.

Arnold, L., Gillet, S., Lardiere, O., Riaud, P. & Schneider, J. (2002). A test for the search for life on extrasolar planets. Looking for the terrestrial vegetation signature in the Earthshine spectrum. *Astron. Astrophys.* **392**, 231–237.

Batalha, N.M. *et al.* (2011). Kepler's first rocky planet: Kepler-10b. *Astrophys. J.* **729**, 27.

Bean, J.L., Miller-Ricci Kempton, E. & Homeier, D. (2011). *Nature* **468** (7324), 669.

Bonfils, X. *et al.* (2005). *Astron. Astrophys.* **443**, L15.

Borucki, W.J. *et al.* (2011). Characteristics of planetary candidates observed by Kepler. II. Analysis of the first four months of data. *Astrophys. J.* **736**, 19.

Brack, A. (1993). Liquid water and the origin of life. In *Origins of Life and Evolution of the Biosphere, 23, 1.* Springer, pp. 3–10.

Charbonneau, D. *et al.* (2009). A super-Earth transiting a nearby low-mass star. *Nature* **462**, 891.

Christensen, P.R. & Pearl, J.C. (1997). Initial data from the Mars Global Surveyor thermal emission spectrometer experiment: observations of the Earth. *J. Geophys. Res.* **102**, 10875–10880.

Cowan, N.B. *et al.* (2009). Alien maps of an ocean-bearing world. *Astrophys. J.* **700**, 915.

Des Marais, D.J., Harwit, M.O., Jucks, K.W., Kasting, J.F., Lin, D.N.C., Lunine, J.I., Schneider, J., Seager, S., Traub, W.A. & Woolf, N.J. (2002). Remote sensing of planetary properties and biosignatures on extrasolar terrestrial planets. *Astrobiology* **2**, 153–181.

Désert, J.-M. *et al.* (2011). Observational evidence for a metal-rich atmosphere on the Super-Earth GJ1214b. *Astrophys. J.*, **731**, 40.

Domagal-Goldman, S.D., Meadows, V.S., Claire, M.W. & Kasting, J.F. (2011). Using biogenic sulfur gases as remotely detectable biosignatures on anoxic planets. *Astrobiology* **11**(5), 419–441.

Fegley, B. & Cameron, A.G.W. (1987). A vaporization model for iron/silicate fractionation in the Mercury protoplanet. *Earth Planet. Sci. Lett.* **82**, 207.

Gaidos, E. & Williams, D.M. (2004). Seasonality on terrestrial extrasolar planets: inferring obliquity and surface conditions from infrared light curves. *New Astron.* **10**, 67–72.

Grasset, O., Schneider, J. & Sotin, C. (2009). *Astrophys. J.* **693**, 722.

Grenfell, J.L., Stracke, B., von Paris, P., Patzer, B., Titz, R., Segura, A. & Rauer, H. (2007). The response of atmospheric chemistry on Earth-like planets around F, G and K Stars to small variations in orbital distance. *Planet. Space Sci.* **55**, 661–671.

Howard Andrew, W., Marcy Geoffrey, W., Bryson Stephen, T., Jenkins Jon, M., Rowe Jason, F., Batalha Natalie, M., Borucki William, J., *et al.* (2011). arXiv:1103.2541.

Kalas, P., Graham, J.R., Chiang, E., Fitzgerald, M.P., Clampin, M., Kite, E.S., Stapelfeldt, K., Marois, C. & Krist, J. (2008). Optical images of an exosolar planet 25 light-years from Earth. *Science* **322**, 1345–1347.

Kaltenegger, L. & Sasselov, D. (2011). Exploring the habitable zone for Kepler planetary candidates. *Astrophys. J.* **736**, L25.

Kaltenegger, L. & Traub, W. (2009). Transits of Earth-like planets. *Astrophys. J.* **698**, 519.

Kaltenegger, L., Segura, A. & Mohanty, S. (2011). Model spectra of the first potentially habitable super-Earth–Gl581d. *Astrophys. J.* **733**, 35.

Kaltenegger, L., Traub, W.A. & Jucks, K.W. (2007). Spectral evolution of an Earth-like planet. *Astrophys. J.* **658**, 598–616.

Kasting, J.F., Toon, O.B. & Pollack, J.B. (1988). How climate evolved on the terrestrial planets. *Sci. Am.* **258**, 90.

Kasting, J.F., Whitmire, D.P. & Reynolds, H. (1993). Habitable zones around main sequence stars. *Icarus* **101**, 108–119.

Kiang, N.Y., Siefert, J.G. & Blankenship, R.E. (2007). Spectral signatures of photosynthesis. I. Review of Earth organisms. *Astrobiology* **7**(1), 222–251.

Lagrange, A.-M. *et al.* (2009). A probable giant planet imaged in the β Pictoris disk. VLT/NaCo deep L′-band imaging. *Astron. Astrophys.* **493**, L21–L25.

Léger, A. *et al.* (2009). Transiting exoplanets from the CoRoT space mission. VIII. CoRoT-7b: the first super-Earth with measured radius. *Astron. Astrophys.* **506**, 287.

Lissauer, J.J. *et al.* (2011). Architecture and dynamics of Kepler's candidate multiple transiting planet systems. *Astrophys. J.* **197**, 8.

Livengood, T.A. *et al.* (2011). Properties of an Earth-like planet orbiting a Sun-like star: Earth observed by the EPOXI mission. *Astrobiology* **11**, 907.

Lovelock, J.E. (1975). Thermodynamics and the recognition of alien biospheres. *Proc. R. Soc. Lond., Series B, Biol. Sci.* **189**(1095), 167–180.

Marois, C., Macintosh, B., Barman, T., Zuckerman, B., Song, I., Patience, J., Lafrenière, D., Doyon, R. *et al.* (2008). Direct imaging of multiple planets orbiting the star HR 8799. *Science* **322**, 1348–1350

Meadows, V. & Seager, S. (2010). Terrestrial planet atmospheres and biosignatures. In *Exoplanets*, ed. Seager, S. & Tucson, A.Z., Tucson, AZ, USA, pp. 441–470. University of Arizona Press, 2010, 526 pp. ISBN 978-0-8165-2945-2.

Miguel, Y., Kaltenegger, L., Fegley, B. & Schaefer, L. (2011). Compositions of hot super-Earth atmospheres: exploring Kepler candidates. *Astrophys. J. Lett.* **742**, L19.

Miller-Ricci Kempton, E., Zahnle, K. & Fortney, J.J. (2012). The atmospheric chemistry of GJ 1214b: photochemistry and clouds. *Astrophys. J.* **745**, 3.

Montanes-Rodriguez, P., Pallé, E. & Goode, P.R. (2007). Measurements of the surface brightness of the Earthshine with applications to calibrate lunar flashes. *Astrophys. J.* **134**, 1145–1149.

Montañés-Rodriguez, P., Pallé, E., Goode, P.R., Hickey, J. & Koonin, S.E. (2005). Globally integrated measurements of the Earth's visible spectral albedo. *Astrophys. J.* **629**, 1175–1182.

Moskovitz, N.A., Gaidos, E. & Williams, D.M. (2009). The effect of Lunarlike satellites on the orbital infrared light curves of Earth-analog planets. *Astrobiology* **9**(3), 269–277.

Pallé, E., Ford Eric, B., Seager, S., Montañés-Rodríguez, P. & Vazquez, M. (2008). Identifying the rotation rate and the presence of dynamic weather on extrasolar Earth-like planets from photometric observations. *Astrophys. J.* **676**, 1319–1329.

Pallé, E., Zapatero Osorio, M.R., Barrena, R., Montañés-Rodríguez, P. & Martín, E.L. (2009). Earth's transmission spectrum from lunar eclipse observations. *Nature* **459**, 814–816.

Pavlov, A.A., Hurtgen, M.T., Kasting, J.F. & Arthur, M.A. (2003). Methane-rich proterozoic atmosphere? *Geology* **31**, 87–92.

Pavlov, A.A., Kasting, J.F., Brown, L.L., Rages, K.A., Freedman, R. & Greenhouse, R. (2000). Greenhouse warming by CH_4 in the atmosphere of early Earth. *J. Geophys. Res.* **105**, 981–992.

Pierrehumbert, R. & Gaidos, E. (2011). Hydrogen greenhouse planets beyond the habitable Zone. *Astrophys. J.* **734**, 13L.

Sagan, C., Thompson, W.R., Carlson, R., Gurnett, D. & Hord, C. (1993). A search for life on Earth from the Galileo spacecraft. *Nature* **365**, 715.

Scalo, J. *et al.* (2007). *Astrobiology* **7**, 85.

Schaefer, L. & Fegley, B. (2004). A thermodynamic model of high temperature lava vaporization on Io. *Icarus* **169**, 216.

Schaefer, L. & Fegley, B. (2009). Chemistry of silicate atmospheres of evaporating Super-Earths. *Astrophys. J. Lett.* **703**, L113.

Schindler, T.L. & Kasting, J.F. (2000). Synthetic spectra of simulated terrestrial atmospheres containing possible biomarker gases. *Icarus* **145**, 262–271.

Schopf, J.W. (1993). Microfossils of the Early Archean Apex Chert: new evidence of the antiquity of life. *Science* **260**, 640–642.

Seager, S. & Ford, E.B. (2002). The vegetation red edge spectroscopic feature as a surface biomarker. In *Astrophysics of Life Conference Proceedings, STScI*, May 2002, 9 pages. arXiv:astro-ph/0212550.

Seager, S., Kuchner, M., Hier-Majumder, C.A. & Militzer, B. (2007). Mass-radius relationships for solid exoplanets. *Astrophys. J.* **669**, 1279–1297.

Seager, S., Turner, E.L., Schafer, J. & Ford, E.B. (2005). Vegetation's red edge: a possible spectroscopic biosignature of extraterrestrial plants. *Astrobiology* **5**, 372–390.

Segura, A., Kasting, J.F., Meadows, V., Cohen, M., Scalo, J., Crisp, D., Butler, R.A.H. & Tinetti, G. (2005). Biosignatures from Earth-like planets around M dwarfs. *Astrobiology* **5**, 706–725.

Segura, A., Krelove, K., Kasting, J.F., Sommerlatt, D., Meadows, V., Crisp, D., Cohen, M. & Mlawer, E. (2003). Ozone concentrations and ultraviolet fluxes on Earth-like planets around other stars. *Astrobiology* **3**, 689–708.

Selsis, F. (2000). Review: Physics of Planets I: Darwin and the atmospheres of terrestrial planets. In *Darwin and Astronomy – The Infrared Space Interferometer', Stockholm, Sweden, 17–19 November 1999*, ESA SP 451, Noordwijk, The Netherlands, pp. 133–142.

Selsis, F., Kasting, J.F., Levrard, B., Paillet, J., Ribas, I., Delfosse, X. (2007). A&A, **476**(3), 1373

Sotin, C., Grasset, O. & Mocquet, A. (2007). *Icarus*, 191, 337.

Tinetti, G., Rashby, N. & Yung, Y. (2006). Detectability of red-edge-shifted vegetation on terrestrial planets orbiting M stars. *Astrophys. J. Lett*. **644**, L129–L132.

Traub, W.A. (2003). The Colors of Extrasolar Planets, Scientific Frontiers in Research on Extrasolar Planets, ASP Conference Series, vol. 294, pp. 595–602.

Traub, W.A. (2011). Terrestrial, habitable-zone exoplanet frequency from Kepler. *Astrophys. J*. **745**, 20.

Traub, W.A. & Jucks, K.A. (2006). Possible aeronomy of extrasolar terrestrial planets. In *Atmospheres in the Solar System: Comparative Aeronomy*. Geophysical Monograph 130 ed. Mendillo, M., Nagy, A. & Waite, J.H. American Geophysical Union, Washington, DC, pp. 369–278.

Turnbull, M.C., Traub, W.A., Jucks, K.W., Woolf, N.J., Meyer, M.R., Gorlova, N., Skrutskie, M.F. & Wilson, J.C. (2006). Spectrum of a habitable world: Earthshine in the near-infrared. *Astrophys. J*. **644**, 551–559.

Udry, S. *et al.* (2007). The HARPS search for southern extrasolar planets XI. Super-Earths (5 & 8 M_Earth) in a 3-planet system. *Astron. Astrophys.* **469**, 43.

Valencia, D., Sasselov, D.D. & O'Connell, R.J. (2007). Detailed models of super-Earths: How well can we infer bulk properties? *Astrophys. J*. **665**, 1413.

von Paris, P., Gebauer, S., Godolt, M., Grenfell, J.L., Hedelt, P., Kitzmann, D., Patzer, A.B.C., Rauer, H. & Stracke, B. (2010). The extrasolar planet Gliese 581d: a potentially habitable planet? *Astron. Astrophys.* **522**, 23.

Williams, D.M. & Pollard, D. (2002). *Int. J. Astrobiol*. **1**, 61.

Woolf, N.J., Smith, P.S., Traub, W.A. & Jucks, K.W. (2002). The spectrum of Earthshine: A pale blue dot observed from the ground. *Astrophys. J*. **574**, 430–442.

Wordsworth, R.D., Forget, F., Selsis, F., Millour, E., Charnay, B. & Madeleine, J.-B. (2011). Gliese 581d is the first discovered terrestrial-mass exoplanet in the habitable zone. *Astrophys. J*. **733**, 48.